Efficient modulation cancellation using reflective SOAs

S. Ó Dúill,[1,*] L. Marazzi,[2] P. Parolari,[2] R. Brenot,[3] C. Koos, [1,4] W. Freude,[1,4] and J. Leuthold[1,4]

[1]*Institute for Photonics and Quantum Electronics of the Karlsruhe Institute of Technology, 76131 Karlsruhe, Germany*

[2]*Politecnico di Milano. Dept. Electronics and Information - PoliCom, via Ponzio 34/5, 20133 Milan, Italy*

[3]*III-V Lab, a joint lab of 'Alcatel-Lucent Bell Labs France', 'Thales Research and Technology' and 'CEA Leti', Route de Nozay, 91460 Marcoussis, France*

[4]*Institute for Microstructure Technology of the Karlsruhe Institute of Technology, Hermann-von-Helmholtz-Platz 1, 76344 Eggenstein-Leopoldshafen, Germany*

**sean.oduill@kit.edu*

Abstract: Modulation cancellation and signal inversion are demonstrated within reflective semiconductor optical amplifiers. The effect is necessary to implement colorless optical network units for network end-users, where downstream signals need to be erased in order to reuse the carrier for upstream transmission. The results presented here indicate that reflective semiconductor optical amplifiers possess the perfect high-speed all-optical gain saturation characteristics to completely cancel the downstream modulation at microwatt optical power levels and are thus the prime candidate to be constituents of future optical network units. Theoretical considerations are supported by experiments that show the cancellation of signals with a 6 dB extinction ratio at 2.5 Gbit/s.

OCIS codes: (250.5980) Semiconductor optical amplifiers; (190.5940) Self-action effects.

References and links

1. W. R. Lee, M. Y. Park, S. H. Cho, J. H. Lee, C. Y. Kim, G. Jeong, and B. W. Kim, "Bidirectional WDM-PON based on gain-saturated reflective semiconductor optical amplifiers," IEEE Photon. Technol. Lett. **17**(11), 2460–2462 (2005).
2. E. Wong, K. L. Lee, and T. Anderson, "Low cost WDM passive optical network with directly modulated self-seeding reflective SOA," Electron. Lett. **42**(5), 299–301 (2006).
3. L. Marazzi, P. Parolari, R. Brenot, G. de Valicourt, and M. Martinelli, "Network-embedded self-tuning cavity for WDM-PON transmitter," Opt. Express **20**(4), 3781–3786 (2012).
4. M. Martinelli, L. Marazzi, P. Parolari, M. Brunero, and G. Gavioli, "Polarization in retracing circuits for WDM-PON," IEEE Photon. Technol. Lett. **24**(14), 1191–1193 (2012).
5. K. Sato and H. Toba, "Reduction of mode partition noise by using semiconductor optical amplifiers," IEEE J. Sel. Top. Quantum Electron. **7**(2), 328–333 (2001).
6. E. K. MacHale, G. Talli, P. D. Townsend, A. Borghesani, I. Lealman, D. G. Moodie, and D. W. Smith, "Signal-induced Rayleigh noise reduction using gain saturation in an integrated R-EAM-SOA," Proc. Of Opt. Fiber Comm Conf., Paper O ThA 6, San Diego, (2009).
7. L. W. Casperson and J. M. Casperson, "Power self-regulation in double-pass high-gain laser amplifiers," J. Appl. Phys. **87**(5), 2079–2083 (2000).
8. Z. Liu, M. Sadeghi, G. de Valicourt, R. Brenot, and M. Violas, "Experimental validation of a reflective semiconductor optical amplifier model used as a modulator in radio over fiber systems," IEEE Photon. Technol. Lett. **23**(9), 576–578 (2011).
9. J. Wang, A. Maitra, C. G. Poulton, W. Freude, and J. Leuthold, "Temporal dynamics of the alpha factor in semiconductor optical amplifiers," IEEE J. of Lightw. Tech. **25**(3), 891–900 (2007).
10. A. Naughton, C. Antony, P. Ossieur, S. Porto, G. Talli, and P. D. Townsend, "Optimisation of SOA-REAMs for hybrid DWDM-TDMA PON applications," Opt. Express **19**(26), B722–B727 (2011).

#177114 - $15.00 USD Received 1 Oct 2012; revised 22 Nov 2012; accepted 23 Nov 2012; published 6 Dec 2012

1. Introduction

Reflective semiconductor optical amplifiers (RSOA) have been proposed for use within wavelength division multiplexing passive optical networks (WDM PON) as suitable elements for colorless optical network units (ONU), due to their wideband gain and direct modulation capability [1–3]. Two WDM-PON architectures, which avoid additional seeding light sources, are shown in Fig. 1. In Fig. 1(a) the typical full-duplex wavelength reuse scheme is illustrated: the upstream (US) transmitter exploits a portion of the downstream (DS) signal, coming from the central office/optical line terminal (OLT), as the external seeding source [1]. The ONU RSOA reuses the DS signal for US data transmission back to the OLT. The second architecture, depicted in Fig. 1(b), is the self-seeded configuration [2,3]. In this case, a laser cavity is formed between the ONU RSOA and the Faraday rotating mirror (FRM) at the remote node [4]. The FRM is necessary to unwind the polarization rotation experienced by the laser field over a complete round-trip of the long cavity. It should be noted that the cavity incorporates the distribution fiber and the arrayed waveguide grating (AWG), which acts as the wavelength selective element. RSOA gain compression is key to implementing ONUs using both of these configurations because of the necessity to reduce the signal extinction ratio (ER) of the downstream signal (recirculating signal in the self-seeded case) in order to make it reusable for upstream transmission. The outgoing (US) lightwave then may be re-modulated with new information. For the case of externally seeded WDM PONs the RSOA could, for instance, amplify and squeeze the transmitted downstream signal [1]. For the self-seeded WDM PON [2,3], the unwanted modulation of the re-circulating signal in the cavity is squeezed.

Signal squeezing in an RSOA is key to suppressing any modulation and to restore a cleaned-up optical carrier for re-use within WDM PON systems. A simplified schematic of desired modulation cancelation along with the direction and position of the input and output waveforms are shown in Fig. 1(c). Up to now, analysis of signal squeezing, under dynamic conditions, has relied upon the well-known single-pass SOA behavior [5]. Signal squeezing experiments using RSOAs for frequency-swept sinusoidal signals [2] and optical noise [6] show strong reduction at low frequencies. The origin of strong squeezing cannot be explained from SOA theory alone. The origin of the strong squeezing results from the unique gain saturation properties of RSOAs. The main difference between the gain saturation of RSOAs and SOAs is that the SOA is effectively a single-pass amplifier whose gain saturates monotonically, with increasing optical power, along the length of the device; whereas in the RSOA a percentage of the light at the reflecting facet is traveling back through the amplifier. As a consequence, the forward and backward traveling waves compete for gain from the same source of carriers, and due to this feedback process the gain saturates more strongly. An approximate analytic approach to calculate the static gain saturation of generalized reflective amplifiers was presented in [7]. For low values of reflectivity, < 50%, there exists a local maximum in the output power with respect to the input power. The existence of a local maximum in the output power creates the condition for strong signal squeezing because power variations in the input signal are not transferred to the output signal.

#177114 - $15.00 USD Received 1 Oct 2012; revised 22 Nov 2012; accepted 23 Nov 2012; published 6 Dec 2012

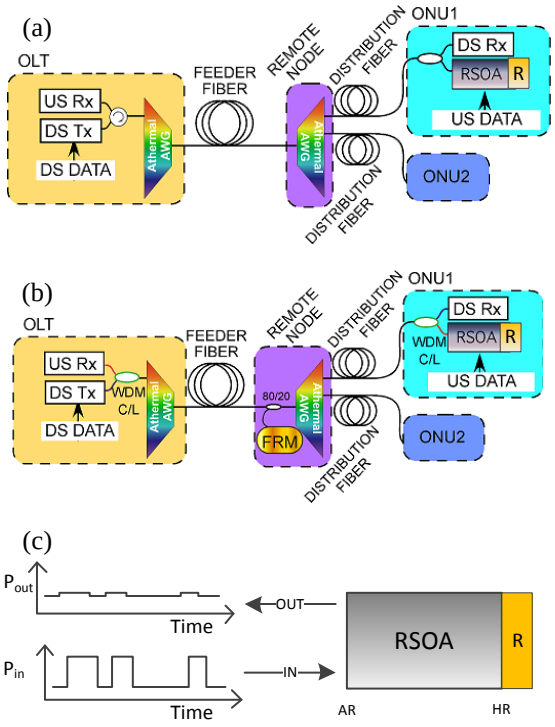

Fig. 1. Illustrations of typical WDM-PON architectures, showing the positioning of RSOAs within the ONUs, for: (a) externally seeded and (b) self-seeded configurations. An illustration of modulation cancellation using the RSOA is depicted in (c). Acronyms: OLT optical line terminal, US upstream, DS downstream, Rx receiver, Tx transmitter, ONU optical network unit, anti-reflection (AR), high-reflection (HR).

In this paper we investigate in detail, showing supporting experimental and numerical results, the modulation cancellation properties of RSOAs under dynamic conditions at 2.5 Gbit/s. A spatially resolved, dynamic RSOA model incorporating carrier injection, spontaneous carrier recombination, stimulated emission due to counter-propagating optical signals with amplified spontaneous emission (ASE) and internal scattering losses was developed to obtain the numerical results. The dynamic model is necessary to show the transients that appear in the output signal. We show how the modulation component of the signal travelling in the DS direction can be completely cancelled using the unique gain saturation behavior of RSOAs. We highlight regimes of operation where the modulation component of the output signal is (a) moderately squeezed (b) exactly cancelled (c) inverted. The inverted regime occurs when the output power decreases with increasing input power [7] and is termed here as signal self-inversion because the strong self-gain saturation causes the residual modulation on the outgoing wave to be an inverted copy of the incoming modulation. As a consequence of this signal self-inversion effect, there exists an optimal input optical power to achieve modulation cancellation in RSOAs. For RSOAs this optimum power levels is achieved at sub-milliwatt power levels, thus making this approach quite attractive for extended reach PONs. Finally, as a by-product of this research, our results show that under the condition of perfect cancellation, the RSOA performs an exact all-optical time differentiation of the intensity signal due to the strong gain saturation under dynamic conditions.

2. Numerical modeling of RSOAs

The employed RSOA is a 800 μm long device with a far-facet reflectivity of 10% driven at a constant bias current of 190 mA [8]. The experimental setup and simulation framework are

#177114 - $15.00 USD Received 1 Oct 2012; revised 22 Nov 2012; accepted 23 Nov 2012; published 6 Dec 2012

shown in Figs. 2(a) and 2(b) respectively. The static experiments were conducted without modulation. The input power was varied using a variable optical attenuator and the RSOA input and output powers were registered via optical power meters.

The spatially resolved simulations modeled both counter-propagating waves within the RSOA, and regarded dynamic carrier injection [8,9]. The modeling framework for the RSOA is similar to that of single-pass SOAs with the appropriate boundary conditions applied at the reflective facet. The RSOA gain is determined by the injected charged carriers into the active region:

$$\frac{\partial N(z,t)}{\partial t} = \frac{I_{RSOA}(z,t)}{eV} - R_{spon}(z,t) - R_{stim}(z,t) \tag{1}$$

where: z and t are the spatial and temporal variables respectively; N is the carrier density; I_{RSOA} is the injected current into the RSOA; e is the unit of elementary electronic charge; V is the volume of the active RSOA gain region; R_{spon} is the rate of spontaneous emission and R_{stim} is the rate of stimulated emission. The rate of stimulated emission is given by:

$$R_{stim}(z,t) = \frac{\Gamma a\left(N(z,t)-N_0\right)}{1+\varepsilon_{nl}P_{tot}(t)} \frac{\left[\left|E^+(z,t)\right|^2+\left|E^-(z,t)\right|^2+\varepsilon^+(z,t)+\varepsilon^-(z,t)\right]}{wdh\upsilon} \tag{2}$$

where: Γ is the confinement factor of the light in the active region; a is the differential gain, N_0 is the carrier density at transparency; ε_{nl} is the nonlinear gain compression factor; wd is the area of the active region; $h\upsilon$ is the photon energy; $E^{\pm}$ represents the optical field of the counter-propagating optical signal with the directions defined in Fig. 2(b); $\varepsilon^{\pm}$ represents the power of the propagating ASE in the RSOA; P_{tot} is the total power of the counter-propagating optical signal and ASE. The rate of spontaneous emission is given by:

$$R_{spon}(z,t) = AN(z,t) + BN^2(z,t) + CN^3(z,t) \tag{3}$$

where, A is the rate of nonradiative recombination; B is the rate of bimolecular recombination and C is the rate of Auger recombination.

The equations for the propagation of the counter-propagating fields are given by:

$$\frac{\partial E^{\pm}(z,t)}{\partial z} \mp \frac{1}{v_g}\frac{\partial E^{\pm}(z,t)}{\partial t} = \frac{1}{2}E^{\pm}(z,t)\left[-\gamma_{\text{int}} + (1-j\alpha_{LE})\frac{\Gamma a(N(z,t)-N_0)}{1+\varepsilon_{nl}P_{tot}(t)}\right] \tag{4}$$

where v_g is the group velocity; γ_{int} is the internal scattering loss of the RSOA waveguide; α_{LE} is the linewidth enhancement factor. The RSOA boundary conditions (BC) are that the input lightwave to the RSOA is always known at all times, i.e. $E^+(0,t) = E_{in}(t)$. At the reflective facet the BC is given by $E^-(L,t) = \sqrt{R}E^+(L,t)$, with R being the reflectivity. For a given input, $E^+(0,t)$, the output lightwave $E^+(0,t)$ is calculated using Eq. (1) and Eq. (4) by employing the techniques outlined in [8,9] and applying the RSOA boundary conditions. The RSOA input, $E^+(0,t)$, and output, $E^-(0,t)$, lightwaves can only be measured in fiber, therefore an additional fiber-RSOA coupling loss is used to determine the fiber-coupled input and output lightwaves at the RSOA input (AR) facet.

The static RSOA gain versus input power characteristic and the output power versus input power of an RSOA are shown in Figs. 2(c) and 2(d). The measured results (open circles) are

#177114 - $15.00 USD Received 1 Oct 2012; revised 22 Nov 2012; accepted 23 Nov 2012; published 6 Dec 2012

plotted along with the simulation results (solid lines). The RSOA device parameters used are shown in Table 1.

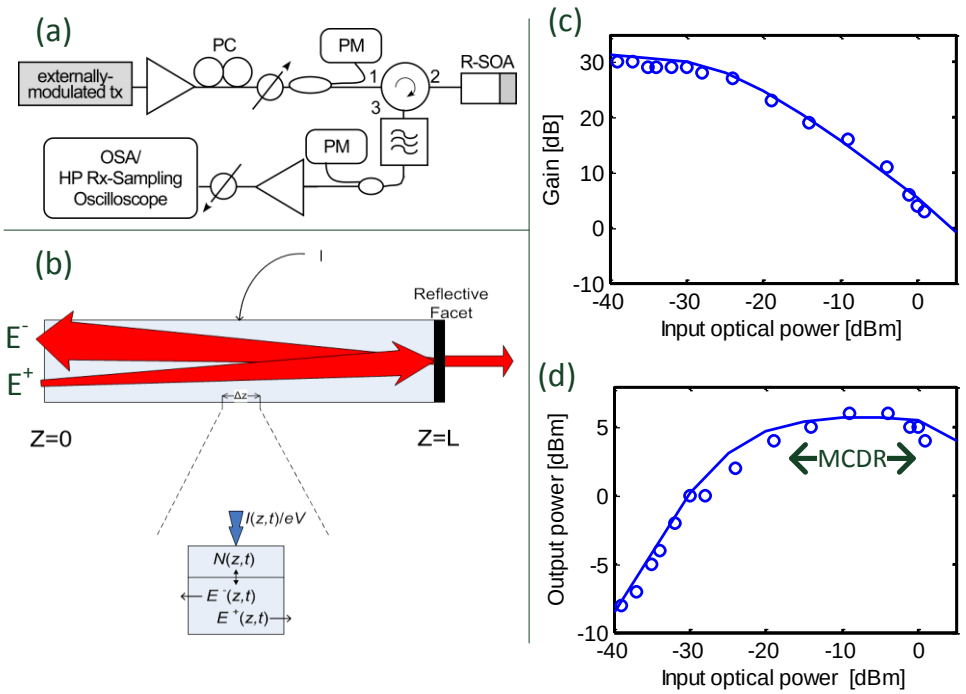

Fig. 2. (a) Experimental setup. Acronyms: PC polarization controller, PM power meter, OSA optical spectrum analyser. (b) Simulation framework to calculate the spatially resolved carrier density profile and counter-propagating waves. (c) Static fiber coupled- RSOA gain versus input power. (d) Static input power - output power transfer characteristic. Within (c) and (d): Open circles denote experimental results, solid lines denote simulation result. MCDR: Modulation cancellation dynamic range

The RSOA shows extremely large, > 30 dB, unsaturated fiber-coupled gain which reduces by 3 dB from peak gain occurring at input powers as small as –27 dBm. Such strong levels of gain saturation at low input power are only possible due to the gain saturation caused by the backwards traveling wave within RSOAs. Because of the strong gain saturation, the RSOA experiences a large gain reduction by 28 dB at an input power of about 0 dBm. Further increases in input power results in such a large gain saturation that the output power decreases with increasing input power, this is consistent with the results in [7,10]. To illustrate this point further, the steady-state, spatially resolved counter-propagating waves and carrier densities are plotted in Fig. 3. In Fig. 3(a) the power of the travelling waves, with –6 dBm input power, are plotted. Owing to the strong depletion of carriers at the input anti-reflection (AR) facet, amplification takes place close to the high reflection (HR) facet where the carrier density is higher. Note that the actual power of the travelling waves within the RSOA are plotted in Fig. 3(a), this number includes the 6 dB coupling loss between the fiber and RSOA. Steady-state carrier density profiles are plotted in Fig. 3(b) at different input powers, –15 dBm, –6 dBm and 2 dBm. Note that the carrier density is almost constant at positions close to the AR facet irrespective of the input power. Strong reduction in carriers close to the HR facet is observed for input powers increasing from –15 dBm to 2 dBm.

.

#177114 - $15.00 USD Received 1 Oct 2012; revised 22 Nov 2012; accepted 23 Nov 2012; published 6 Dec 2012

Table 1. RSOA parameters used in the simulations.

RSOA Parameter	Value	Parameter	Value
RSOA length	800 µm	Confinement factor	20%
Area of Active region	0.18 µm^2	Differential gain	4x10^{-20} m^2
Reflectivity	10%	N_0	5x10^{-23} m^{-3}
A	4x10^8 s^{-1}	B	1x10^{-16} m^{3}s^{-1}
Alpha factor	4	C	1x10^{-42} m^{6}s^{-1}
ε_{nl}	2 W^{-1}	γ_{int}	5,000 m^{-1}
Fiber – RSOA coupling loss	6 dB		

The modulation-cancellation dynamic range (MCDR) is indicated in Fig. 2(d). The MCDR is defined to be the range of input powers, between which there is a less than 1 dB variation in the output power. For the case shown in Fig. 2(d); the MCDR ranges from –15 dBm to –2 dBm. A signal with input powers within the MCDR is compressed to produce a virtually modulation-free continuous wave (CW) output. Its large MCDR, at microwatt levels, makes the RSOA an excellent candidate to perform this modulation-cancellation operation within WDM-PON systems.

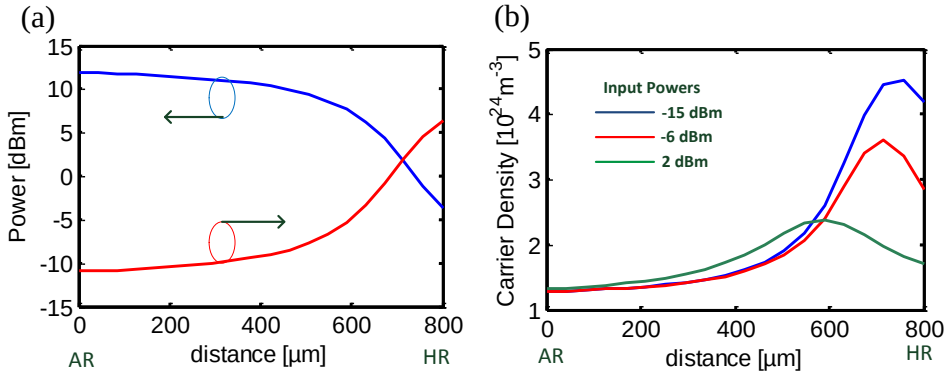

Fig. 3. (a) The steady-state, spatially-resolved power of the travelling waves within the RSOA for a constant input power of – 6 dBm. The red and blue represent the power of the waves travelling to the left and right directions respectively. Note that the fiber-RSOA coupling loss of 6 dB is applied and the red curve begins at –12 dBm. Note that at the HR facet, the blue curve is 10 dB lower than the red curve at this position due to the 10% reflectivity of this facet. (b) Steady state, spatially resolved carrier density profiles along the RSOA for input powers of –15 dBm, –6 dBm and 2 dBm.

3. Modulation cancellation at 2.5 Gbit/s

In the previous section we reported on the response of the SOA for CW optical input signal; however, the RSOA gain depends strongly on the carrier dynamics. Therefore in this section we show results of modulation cancelling experiments at 2.5 Gbit/s.

The experimental setup is shown in Fig. 2(a). The light source is externally modulated while the extinction ratio (ER) of the down-stream signal is held constant at 6 dB. A 2.5 Gbit/s non-return-to-zero (NRZ) optical input signal with ER = 6 dB is launched into the RSOA. The average input power of the signal is controlled using a variable optical attenuator; this allows us to operate on different parts of the RSOA input-output transfer characteristic, Fig. 2(d). The input eyediagram showing the 6 dB ER is shown in Fig. 4 (upper left hand

#177114 - $15.00 USD Received 1 Oct 2012; revised 22 Nov 2012; accepted 23 Nov 2012; published 6 Dec 2012

side). The output eye diagrams for three different input optical powers are also shown in Figs. 4(a)-4(c).

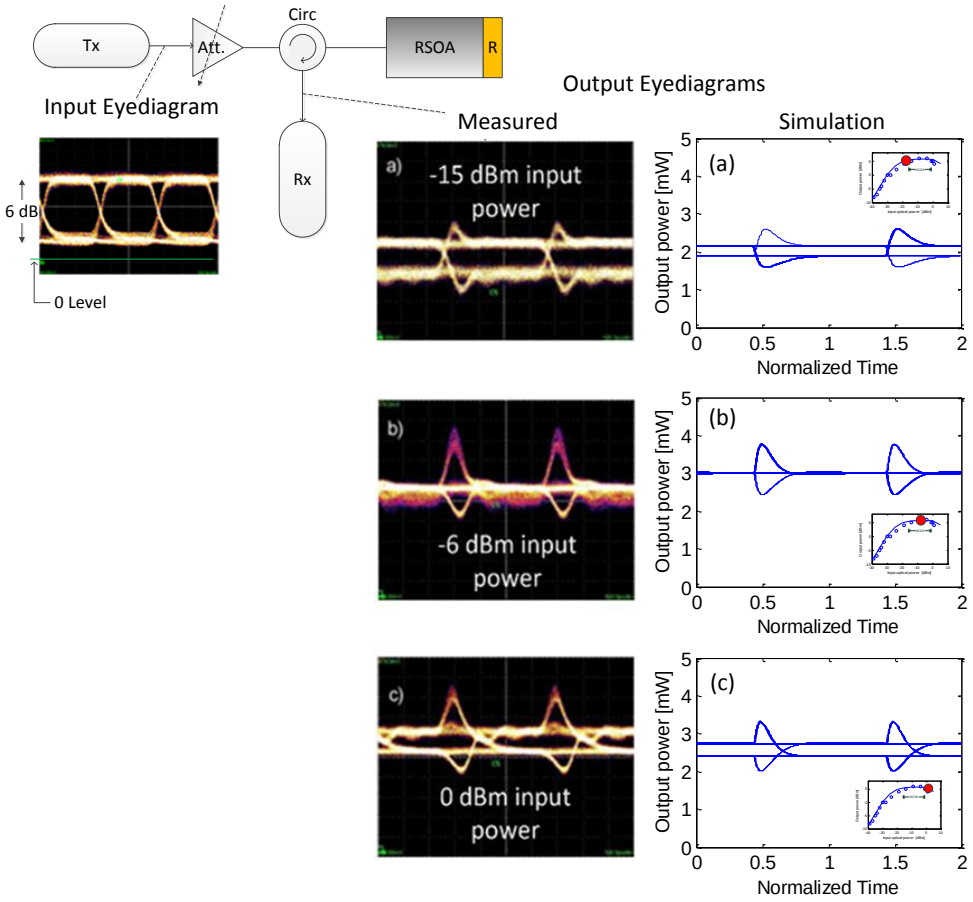

Fig. 4. Modulation cancellation at 2.5 Gbit/s. Experimental and simulated output eyediagrams at 3 different input powers: (a) –15 dBm, (b) - 6 dBm and (c) 0 dBm. The insert within each simulated eyediagram indicates the operating point on the RSOA input-output power transfer characteristic Fig. 2(d). The eyediagram of the input signal with 6 dB ER is shown in the upper left corner. Acronyms: Tx Transmitter, Att Attenuator, Circ circulator, Rx receiver.

At a low input optical power of –15 dBm, Fig. 4(a), signal squeezing is visible; however the modulation is not fully suppressed. At an input optical power of about –6 dBm, Fig. 4(b), the modulation is completely cancelled apart from the presence of transient spikes. The transient spikes occur because the RSOA gain cannot re-adjust instantaneously to variations in the input power. The upward (downward) spikes are created when there is an increase (decrease) in the optical power level. Initially the output power increases (decreases) due to increasing (decreasing) input power, then the gain decreases (increases) due to the altered gain saturation condition. When operated in this condition, the RSOA acts as a perfect time differentiator for the intensity signal. The spikes are undesired for upstream (US) transmission, though they may find use to synchronize the US signal so that the transient spikes occur at the US signal transitions. At higher input powers, greater than 0 dBm, the so-called signal self-inversion is observed; this is depicted in Fig. 4(c). Here, increases in the input power result in a decrease in the output power. In this case the output signal is inverted with respect to the input signal, which is the signal self-inversion effect. Transient spikes are again visible. An upward (downward) spike accompanies an increase (decrease) in the optical

#177114 - $15.00 USD Received 1 Oct 2012; revised 22 Nov 2012; accepted 23 Nov 2012; published 6 Dec 2012

power, though after the transient the optical power attains the lower (upper) level. This effect is unique to RSOA as such behavior cannot be observed in SOAs at input powers as low as 0 dBm.

The gain saturation effects, including the transient spikes, can be also predicted from RSOA simulations. The eye diagrams showing the modulation cancellation for the three different gain compression regions are displayed alongside the experimental results in Figs. 4 (a)-4(c). There is a good agreement between the experimental results and simulations. The simulations show the exact same modulation canceling as the experimental results including the transient spikes and the switching from low to high level after (before) the transient spikes for the case of self-inversion (signal squeezing). Simulations show that in the self-inversion regime, the carrier distribution in the RSOA is heavily depleted at the input and at the reflective facet due to the carrier depletion from the forward and backward traveling waves. The gain depends exponentially [8,9] on the carrier concentration, thus moderate carrier depletion is sufficient to cause a strong reduction in the output power with increasing input power.

4. Optimal operating conditions for modulation cancellation

Figure 5 shows the measured output ER (neglecting the spikes) for different input powers at 1.25 Gbit/s and 2.5 Gbit/s. Clearly the output ER is < 1 dB for input powers between −15 dBm and –2 dBm, the optimal operating power at –6 dBm yields complete cancellation. With increasing input power, the output signal is compressed due to the gain saturation. Once complete cancellation is achieved, the output ER rises again due to the signal self-inversion. This implies an optimal input power level to achieve modulation cancellation using RSOAs.

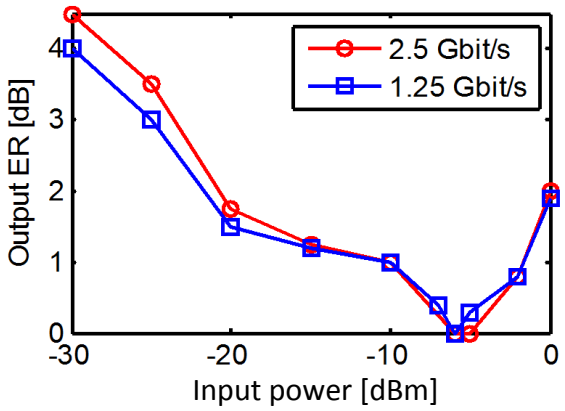

Fig. 5. Measured ER of the output signal as a function of the average input power at 1.25 and 2.5 Gbit/s. The ER a the input is held constant at 6 dB. Ideal cancelation is found for input signal powers of around –6 dBm.

5. Conclusion

We showed detailed corroborative experimental and theoretical results of the RSOA's modulation cancellation function capabilities. Signal squeezing is achieved at low input powers and there exists an optimal input power that completely cancels the incoming modulation. Increases in the input power beyond the optimal point result in signal inversion rather than cancellation.

Acknowledgments

This work was funded by the EU FP7 project ERMES, (GA no. 288542 2012). The online publishing fund of the Karlsruhe Institute of Technology is acknowledged.

#177114 - $15.00 USD Received 1 Oct 2012; revised 22 Nov 2012; accepted 23 Nov 2012; published 6 Dec 2012